X-ray irradiation of graphite solution from carbon rods of zinc-carbon battery wastes assisted by commercial detergent

Cite as: AIP Conference Proceedings **2169**, 060004 (2019); https://doi.org/10.1063/1.5132682
Published Online: 07 November 2019

Wipsar Sunu Brams Dwandaru, Septiana Rahmawati, Rhyko Irawan Wisnuwijaya, Yusman Wiyatmo, Suparno, and Supardi

X-Ray Irradiation of Graphite Solution from Carbon Rods of Zinc-Carbon Battery Wastes Assisted by Commercial Detergent

Wipsar Sunu Brams Dwandaru[a)], Septiana Rahmawati, Rhyko Irawan Wisnuwijaya, Yusman Wiyatmo, Suparno, Supardi

Physics Education Department, Mathematics and Natural Sciences Faculty, Universitas Negeri Yogyakarta, Karangmalang Complex, Yogyakarta, 55281, Indonesia

[a)] Corresponding author: wipsarian@uny.ac.id

Abstract. Graphite solution obtained from a carbon rod of zinc-carbon (ZnC) battery wastes has been irradiated using X-ray in liquid-phase with the assistance of commercial detergent. This study is conducted by preparing graphite and detergent powder, each with an amount of 0.6 grams in 100 ml distilled water. X-ray irradiation with a voltage of 30 kV is performed upon the sample solutions with varying irradiation time durations of 1 hour, 2 hours, and 3 hours. The sample solutions with and without X-ray irradiation are characterized using UV-Visible (UV-Vis) spectroscopy, X-ray diffraction (XRD), scanning electron microscope (SEM), and Fourier transform infrared (FTIR) spectroscopy. The UV-Vis results show decreasing GO absorbance values at a peak of 235 nm after 1 hour of X-ray irradiation. The GO peak disappears for 2 and 3 hours of X-ray irradiation, but a peak at 270 nm occurs indicating an early formation of reduced GO. SEM images show bulky materials before X-ray irradiation and rectangular-like materials after X-ray irradiation. There is a reduction in the sizes of these materials from 4 microns to 2 microns with X-ray irradiation. XRD results show an amorphous phase produced after irradiation. Finally, the FTIR results show similar profiles of the sample solutions for all variations of the irradiation time. The FTIR peaks at 3450 cm^{-1} and 1637 cm^{-1} corresponding to OH and C=C functional groups, respectively, are decreasing at the irradiation time is increased.

INTRODUCTION

Graphene oxide (GO) is a material being intensively studied and largely produced. Although GO is considered as a precursor for producing graphene, the former has many potential applications, such as bio-sensor [1], hydrogen storage [2], and drug deliveries [3]. Further reducing GO produces reduced GO or rGO, which increases the physical properties of GO, especially its electrical properties. GO is synthesized via various methods, e.g. Hummer's method [4], liquid-phase exfoliation [5-7] using a sonicator [8,9] or a blender [10,11], and recently through fluid dynamic route [12].

X-ray is an ionizing radiation that is commonly used for radiology [13], chemotherapy [14], and pipe crack testing [15]. Gamma irradiation has also been used in the reduction of GO into rGO and producing graphene material [16-19]. Gamma irradiation is said to be a greener route [20] giving less pollution compared to other chemically involved methods. In this case, Gamma radiation towards GO will take away the oxygen atoms from the layers and forming cavities [17]. In this case the Hummer's method is commonly used to obtain GO from graphite, which unfortunately involves many chemical compounds that may be hazardous to the environment. In this study, instead of using the Hummer's method, we directly irradiate graphite solution with X-ray radiation in order to produce GO without involving any chemical compounds. The only assisting agent used in order to exfoliate graphene layers is commercial detergent containing about 19% of surfactant. Hence, the objective here is to study the effect of X-ray irradiation towards the exfoliation of graphene layers in the graphite solution assisted by

The 8th National Physics Seminar 2019
AIP Conf. Proc. 2169, 060004-1–060004-9; https://doi.org/10.1063/1.5132682
Published by AIP Publishing. 978-0-7354-1916-2/$30.00

commercial detergent. With the knowledge of the authors, this study has not been conducted before. The X-ray utilized in this study is low energy (soft) X-ray [21], which is used in medical or educational applications.

The main reason in using the graphite solution as a precursor material is because graphite is commonly used to produce GO or rGO as it consists of many graphene layers. Pure graphite material may be obtained by purchasing it. However, the graphite material used in this study is obtained from zinc-carbon (ZnC) batteries wastes. This is beneficial since we use the graphite material, especially the carbon rods, inside the battery wastes. The ZnC battery is one of the widely used primary batteries [22]. This type of battery is still being produced as a power source for various electronic and home appliances such as small radio and TV receivers, clocks, calculators, toys, and so forth. However, ZnC batteries are not rechargeable such that they eventually become wastes. Unfortunately, people tend to be reluctant in recycling and prefer disposing battery wastes. This may cause the water or soil pollutions in the surrounding environment coming from potentially dangerous and toxic metals, such as acid, lead, nickel, lithium, cadmium, and mercury [23]. Hence, it is essential to re-use or recycle ZnC battery wastes in order to prevent the negative effects of the wastes.

METHOD

Materials

The materials used in this study are (i) carbon rods (Fig. 1(b)) from ZnC battery wastes (Fig. 1(a)), (ii) distilled water, and (iii) commercial detergent powder. Moreover, the tools used in this study are (i) a blender, (ii) a measuring glass, (iii) a beaker glass, (iv) sample tubes, (v) a stopwatch, (vi) a digital scale, (vii) aluminium foils, (viii) an X-Ray generator [580 TEL-X-OMETER] (Fig. 2), (ix) UV-Vis spectrophotometer (Shimadzu UV-2550), (x) XRD (Rigaku Miniflex 600), (xi) SEM (CoXem), and FTIR (Nicolet Avatar).

(a) **(b)** **(c)**

FIGURE 1. (a) a used ZnC battery, (b) the carbon rods obtained from the used ZnC battery, and (c) graphite powder obtained from the carbon rods.

Sample Preparation

The carbon rods from the inside of the ZnC battery wastes are collected by breaking open the metal skin of the ZnC batteries. The carbon rods are mashed into powder. An amount of 100 ml distilled water is prepared in a beaker glass. The carbon and detergent powders, each with the same amount of 0.6 grams are poured in the distilled water. The solution is mixed using a blender for two minutes. The graphite-detergent solution is ready to be irradiated.

X-ray Irradiation of the Samples

The X-ray generator used is 580 TEL-X-OMETER, which is a soft X-ray generator. This generator is typically utilized as a practicum or demonstration apparatus for students to show various X-ray applications, e.g.: crystal diffraction and X-ray absorption. The accelerating voltage used is 30 kV, which corresponds to photon energy of

around 20 keV. Moreover, we do not calculate the dose of the X-ray radiation. The main features of interest in this generator are i) the X-ray tube as the source of the X-ray radiation and ii) the material mounts (crystal mount) [Fig. 2] for placing the graphite-detergent solution to be irradiated.

The irradiation preparation process of the carbon material in liquid-phase can be explained as follows. The sample is placed on the crystal mount in front of the X-ray tube (source) with a distance of approximately 1.5 cm (Fig. 3). The aforementioned distance is chosen in order to take into account the fact that this is a soft X-ray that is short ranged, hence providing assurance of X-ray absorption of the graphite solution. A Geiger-Mueller (GM) detector connected to a GM counter is placed on the other end of the graphite solution sample with a distance of 10 cm between the sample and the detector. In order to start the irradiation process, the start button is pressed. If the red light is on, then the X-ray is being produced [Fig. 2(a)].

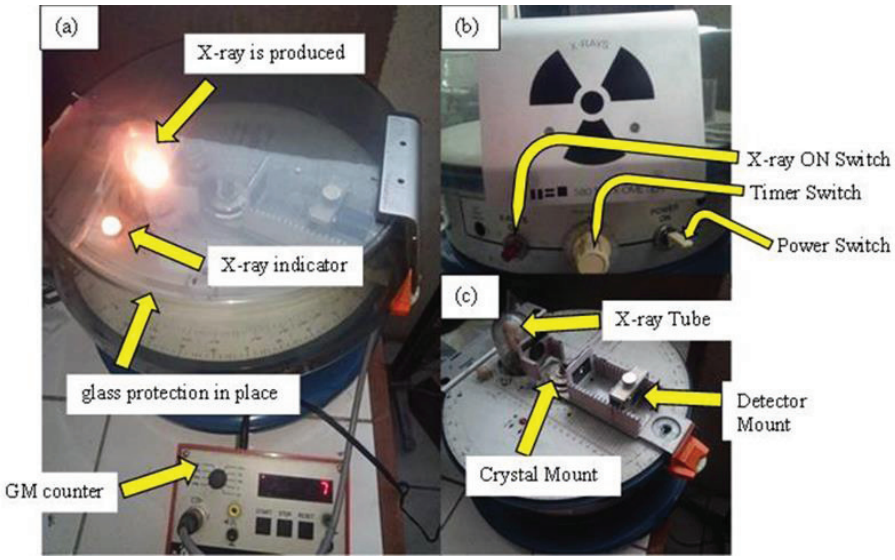

FIGURE 2. Some important features of the 580 TEL-X-OMETER X-ray generator in operational (a) and non-operational [(b)-(c)] modes.

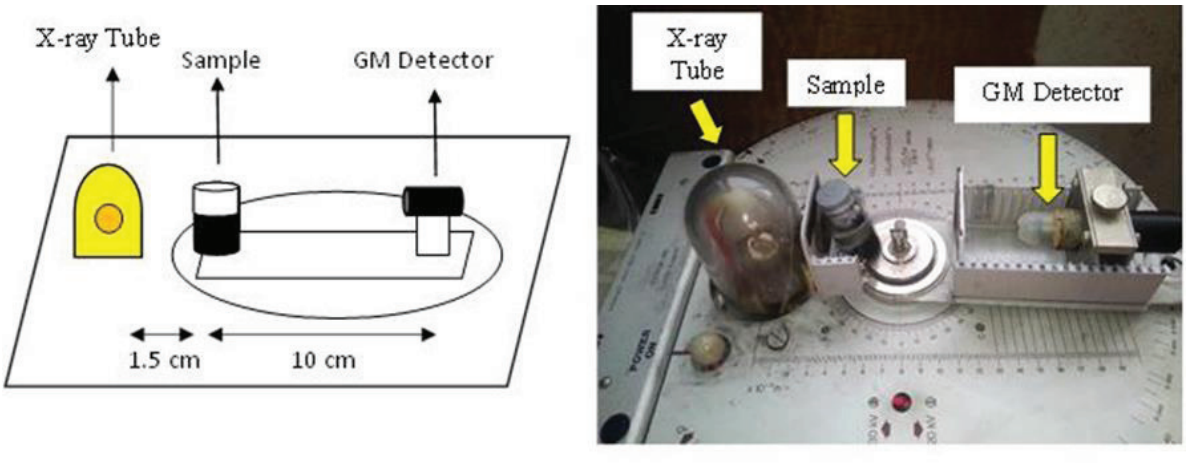

FIGURE 3. A schematic illustration of the graphite-detergent solution irradiation (a) and the actual setup of the graphite-detergent solution on the X-ray generator (b).

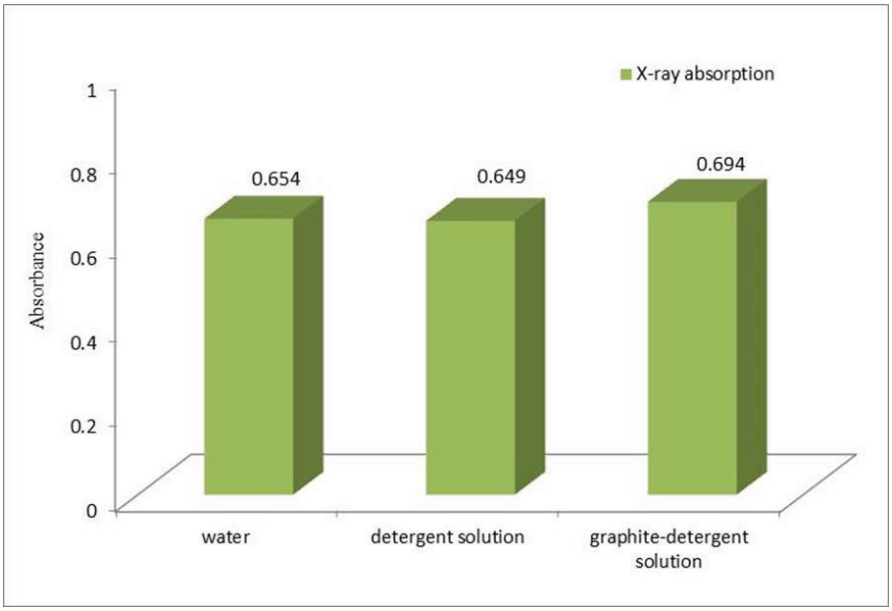

FIGURE 4. The X-ray absorption by various materials, i.e.: (from left to right) distilled water, detergent solution, and graphite-detergent solution.

A preliminary experiment is conducted to determine the absorption of X-ray in the graphite-detergent solution sample. This is done by comparing the GM counter results of the X-ray irradiation for various situations, i.e.: a) without sample, b) sample of distilled water, c) sample of a detergent solution, and d) sample of the graphite-detergent solution. The X-ray generator is set for 55 minutes of irradiation, and the GM counter is set for 30 minutes.

The main experiment is conducted by irradiating the graphite-detergent solution for time durations of (in hours) 1, 2, and 3. After the irradiation process, the sample solutions are then left to equilibrate for a night. The results of the sample solutions may be observed in Fig. 5. Finally, the sample solutions are then ready to be characterized.

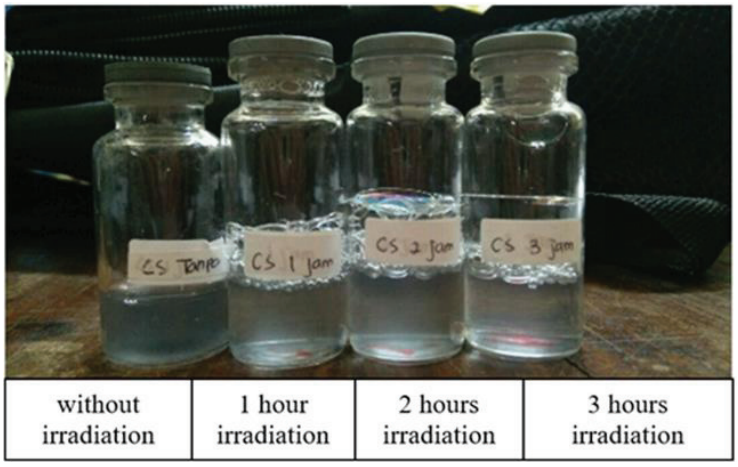

FIGURE 5. The graphite-detergent solution samples with and without X-ray irradiation.

Characterization of the Samples

Subsequently, the samples are characterized. UV-Vis spectroscopy and FTIR are conducted in liquid-phase, whereas XRD and SEM are done in solid-phase. The solidified samples are obtained by dip coating glass slides upon the surface of the sample solution and then heating the glass slides in an oven for 10 minutes at a temperature of 250 ºC. In this study, downsizing is conducted upon the type and number of the samples being characterized. Based upon Fig. 5 there are four samples that are characterized using the UV-Vis spectrophotometer, i.e.: samples with 1, 2, and 3 hours of X-ray irradiation and without irradiation. For the FTIR characterization we conducted the test upon all the samples with X-ray irradiation, but leave out the sample without irradiation. Finally, for the XRD and SEM characterizations we only conducted the tests for samples with 3 hours of X-ray irradiation and without irradiation. This is done, as there is a limitation in the funding of the study.

RESULT AND DISCUSSION

The X-ray irradiation count measured from the X-ray generator is 6,276 count per hour. The sample solutions without and with X-ray irradiation assisted by commercial detergent may be observed in Fig. 5. The leftmost sample is the solution without irradiation. The second, third, and fourth samples (from the left) are resulted from 1 hour, 2 hours, and 3 hours of X-ray irradiation. It may be observed that the sample without X-ray irradiation is murkier compared to the samples with X-ray irradiation. However, there is no physical difference of the samples with varying time of X-ray irradiation. All samples are perceived murky, which might be caused by the detergent content in the samples.

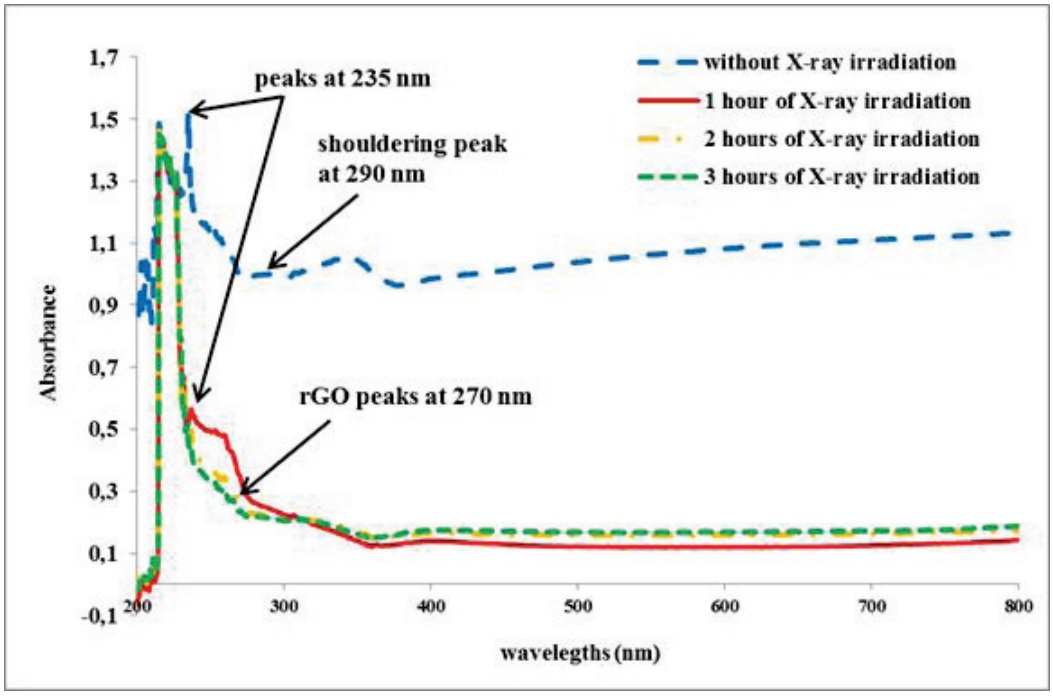

FIGURE 6. The UV-Vis results of the sample solutions without and with X-ray irradiation.

The UV-Vis characterization results of the samples may be observed in Fig. 6. The samples without X-ray irradiation, 1 hour, 2 hours, and 3 hours of X-ray irradiation are represented by dashed (blue), solid (red), dashed-dotted (yellow), short-dashed (green) lines, respectively. The UV-Vis results for the sample without X-ray irradiation shows peaks at 235 nm and a shouldering peak at 290 nm, which correspond to the $\pi \rightarrow \pi^*$ and $n \rightarrow \pi^*$

electronic transitions, respectively. Hence, indicating the formation of the GO from the graphite solution. This is caused by the graphite carbon powder exfoliation by the surfactant in the detergent. The surfactant moves in between the graphene layers in the graphite making the distance between adjacent graphene layers to increase, hence forming GO. The treatment of X-ray irradiation clearly decreases the absorbance of the sample solutions, especially at the peak of 235 nm. For 1 hour of irradiation, an absorbance decrease of the sample solution is clearly observed at the peak of 235 nm. This means that the amount of GO is reduced by the irradiation. Moreover, for 2 and 3 hours of irradiation a small peak at 270 nm starts to occur, which indicates an early formation of rGO obtained from the reduction of GO caused by X-ray irradiation. However, it seems that there is still a small amount of rGO formed based on the low absorbance value at the peak of 270 nm in accordance with Otari, *et al*. (2017) and Derkaoui, *et al.* (2016).

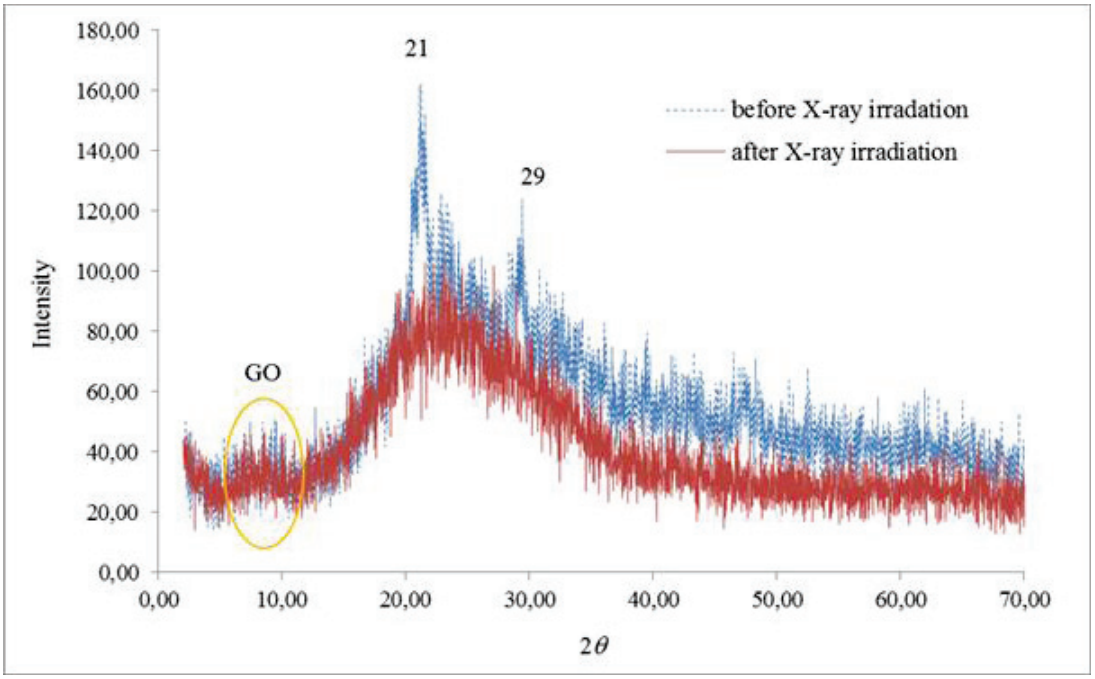

FIGURE 7. XRD results of the solidified sample solutions with (solid-red pattern) and without (dashed-blue pattern) X-ray irradiation.

The XRD characterizations of the sample solutions with and without X-ray irradiation are given in Fig. 7. The solution used for XRD characterization is the sample with 3 hours of X-ray irradiation. It may be observed that without X-ray irradiation the sample shows a crystalline pattern with two prominent peaks at 21° and 29°. There is also a small bump around 10°, which signifies the presence of GO material in the sample solution. However, the sample solution with X-ray irradiation tends to become amorphous as no peaks are observed in the XRD data. Moreover, the intensity of the XRD data is reduced to the sample solution with X-ray irradiation. This shows that X-ray irradiation tends to destroy the crystallinity of the sample solution. The amorphous state of the sample is in accordance to the SEM results in Fig. 8(b). The GO peak at 10° in the XRD sample solution with X-ray irradiation supports the UV-Vis results that GO is still present in the solution, transforming towards rGO in accordance with Rajagopalan and Chung (2014).

The SEM results of the solidified sample with and without X-ray irradiation may be observed in Fig. 8. In this case, we use again the sample solution with 3 hours of X-ray irradiation to be characterized. Fig. 8(a) shows the surface morphology image of the sample solution without X-ray irradiation compared to Fig. 8(b), which shows the image of the sample solution with X-ray irradiation with magnification of 10,000X. Fig. 8(a) clearly shows bulky materials (inside the yellow circle). The sizes of these materials are around 4 microns. Different result occurs in the surface morphology of the sample after being subjected to X-ray irradiation, which is evident in the presence of smaller widths of rectangular-like materials. This indicates an exfoliation of bulk materials (without irradiation) into

smaller materials. The sizes of these rectangular-like materials are around 2 microns (Fig. 8(b)). Hence, there is a decrease in the material size without and with the X-ray irradiation, hence indicating that the irradiation reduces the size of the materials. Furthermore, the materials seem to be homogeneously scattered throughout the sample and have a hollow center. This is in accordance with the findings of Dumée (2014) that cavities occur when GO is irradiated with X-ray as the oxygen is taken away from the GO layers. Furthermore, Fig. 8(b) suggests that the X-ray irradiation treatment reduces the widths of these rectangular-like materials.

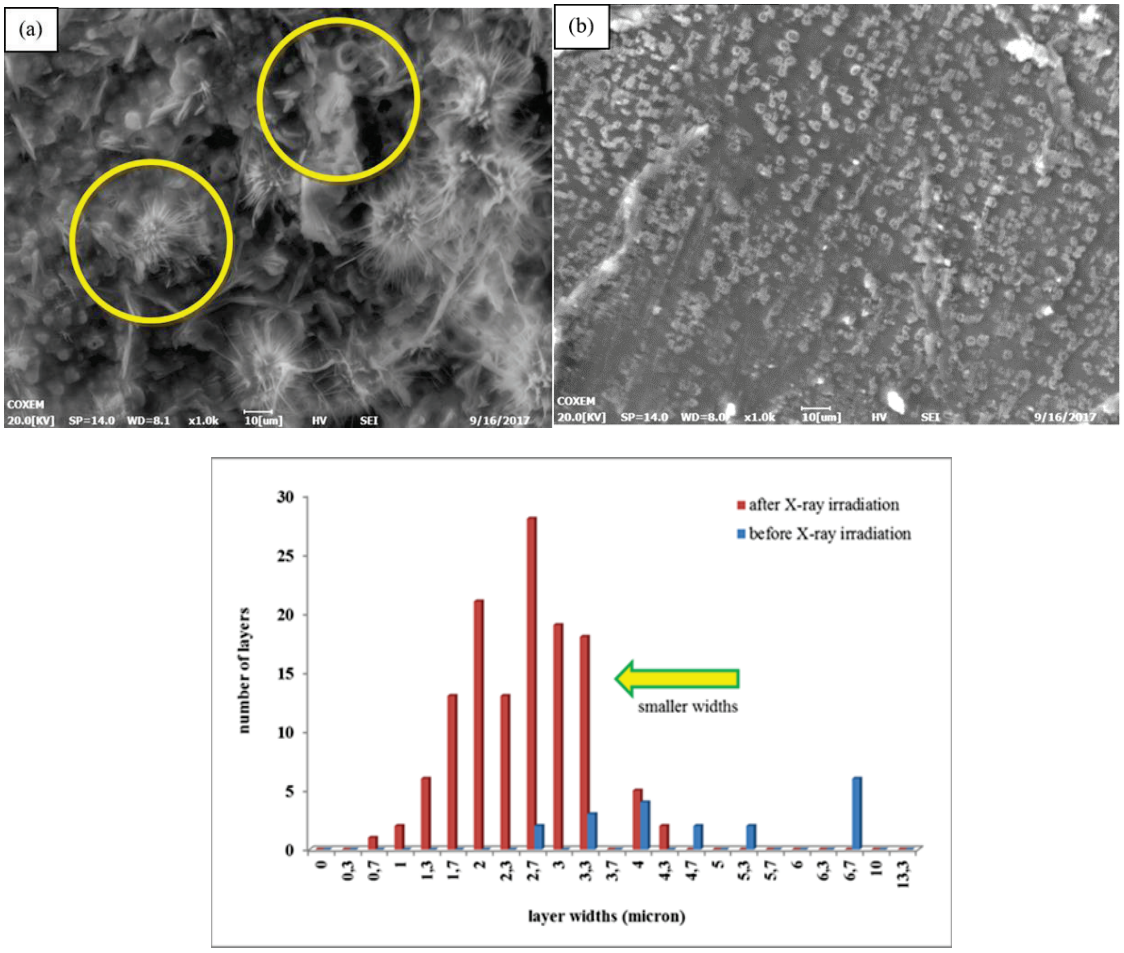

FIGURE 8. SEM images of the sample solutions without (a) and with (b) X-ray irradiation with magnification of 10,000x Layer width distribution (bottom figure) of the sample solution with (red) and without (blue) X-ray irradiation.

The FTIR results of the samples with X-ray irradiation may be observed in Fig. 9. The figure shows FTIR profiles of the sample solutions with X-ray irradiation time exposures of 1 hour (dash-dotted line), 2 hours (solid line), and 3 hours (dashed line). In general, the three profiles appear to be similar with similar peak locations. However, for 2 hours of irradiation there is a peak, which is not present in the two other profiles, that is at a wave number of 2,361 cm^{-1}, which indicates a CO2 functional group. The three profiles are in accordance with the FTIR profile of GO. A deep but wide peak occurs at around 3,450 cm^{-1} showing an OH functional group. The blue arrow indicates a reduction of the transmittance at the irradiation time is increased from 1 hour to 3 hours. This is consistent with the UV-Vis results of the reduction of GO into rGO. However, this decrease is still small and seems to be linear with respect to the irradiation time. Hence, 3 hours of X-ray irradiation is not enough to fully reduce GO into rGO. Alkynes functional group is obtained around the peak of 2,070 cm^{-1}. Double bond of carbon atoms is realized at the peak of 1,637 cm^{-1} indicating the existence of the hexagonal carbon structure of the graphene layer.

The transmittance of these peaks seems to decrease as the irradiation time is increased. This may contribute to the effect of the X-ray in creating a hollow or cavity region observed in the SEM result of Fig. 8(b). Finally, small peaks at around 1,378 cm^{-1} and 1,089 cm^{-1} are observed showing the presence of C-O functional groups.

The solution that consists of distilled water, graphite powder, and detergent powder produces GO solution that causes the insertion of oxygen atom, e.g.: OH and COOH molecules, into the graphene layers of the graphite as shown from the FTIR results in Fig. 9. Moreover, the surfactant molecules move into the gap between two adjacent graphene layers, causing the distance increase of the adjacent graphene layers. The X-ray irradiation towards the solution causes radiolysis of water, hence reducing the H_2O molecules, as electrons are being ionized or excited. These free electrons may be absorbed by the graphite or react with water molecules. Water radiolysis produces radical ions, such as OH^- and H^+. The H^+ ions which are located around the region between graphene layers further increase the repulsive interactions between the hydrophilic heads of the detergent, hence further exfoliating the graphite into GO. The X-ray irradiation may also ionize oxygen atoms directly from the GO layers such that cavities occur (Dumée, 2014) hence reducing the crystallinity of GO in accordance with the XRD results in Fig. 7. The interaction between the X-ray with the graphite may also disrupt the attachment between the tails of the detergent with the graphene layers, such that separation between graphene layers occurs.

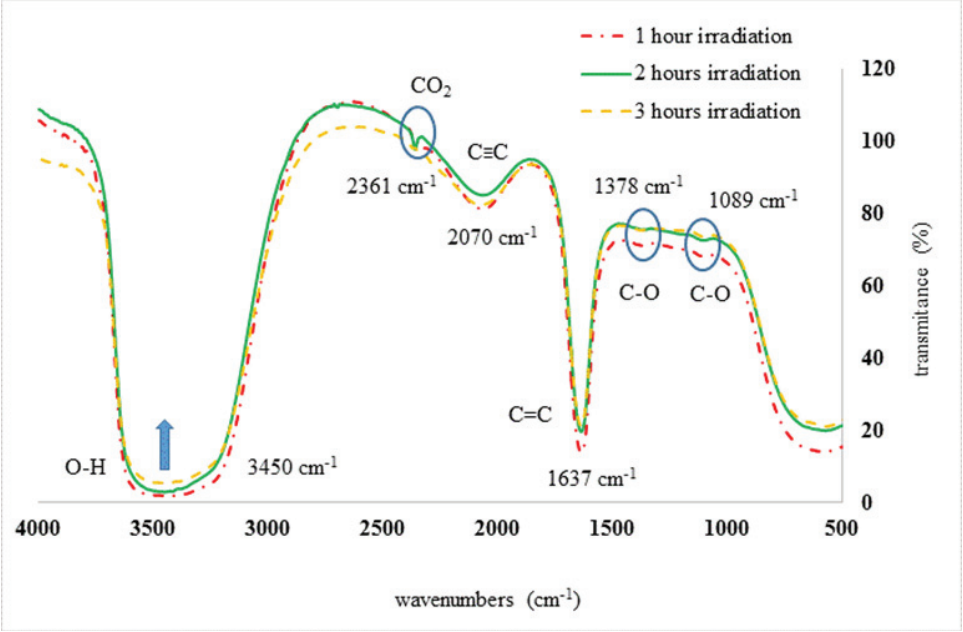

FIGURE 9. FTIR results of the samples with X-ray irradiation time exposures of 1 hour (dash-dotted red line), 2 hours (solid-green line), and 3 hours (dashed-yellow line).

CONCLUSION

X-ray irradiation has been conducted on graphite solution from carbon rods of use ZnC batteries assisted by commercial detergent. The time duration of the X-ray irradiation is varied from 1 hour to 3 hours. The UV-Vis result shows that GO is produced in the sample solution without X-ray irradiation, which is caused by exfoliation of the graphene layers by surfactants in the detergent. The UV-Vis results of the samples with X-ray irradiation show a decreasing absorbance values and the occurrence of a peak at 270 nm, especially for 2 and 3 hours of X-ray irradiation. This suggests an early formation of rGO. The SEM images show bulky materials of the sample without X-ray irradiation and small rectangular-shaped materials with X-ray irradiation. There is a reduction in the size of the materials going from without to with X-ray irradiation that is from 4 microns to 2 microns. The XRD results show an amorphous phase of the GO materials with X-ray irradiation. Finally, the FTIR results show functional groups belonging to GO with similar profiles for all variations of X-ray irradiation time. The X-ray irradiation upon

the sample solution decreases the OH functional group of the GO, but not enough to fully reduce GO into becoming rGO.

ACKNOWLEDGEMENTS

The authors would like to thank the Faculty of Mathematics and Natural Science, Universitas Negeri Yogyakarta for funding this research under the Faculty Research Group scheme with contract number of 94/Research Group/34u/11/2018.

REFERENCES

1. A.J. Haes and R. P. Van Duyne, *J. Am. Chem. Soc* ***124***, 10596(2002).
2. R. Nagar, B.P. Vinayan, S.S. Samantaray and S. Ramaprabhu, *J. Mater. Chem. A* ***5***, pp. 22897-22912(2017).
3. T. Yin, J. Liu, Z. Zhao, Y. Zhao, L. Dong, M. Yang and J. Zhou, *Adv. Funct. Mater.* ***27(14)***, 1604620(2017).
4. N. Justh, B. Berke, K. Laszlo and I. M. Szilagyi, *J. Therm. Anal. Calorim* ***131(3)***, pp. 2267-2272(2018).
5. A. Ciesielski and P. Samori, Chem. Soc. Rev **43**, 381 (2014).
6. Y. Hernandez, V. Nicolosi, M. Lotya, F. Blighe, Z. Sun, S. De, I.T. McGovern, B. Holland, M. Byrne, Y. Gunko, J. Boland, P. Niraj, G. Duesberg, S. Krishnamurti, R. Goodhue, J. Hutchison, V. Scardaci, A.C. Ferrari and J.N. Coleman, *Nat. Nanotechnol* ***3***, pp. 563-568(2008).
7. J.N. Coleman, M. Lotya, A. O'Neil, S.D. Bergin, P.J. King, U. Khan, K. Young, A. Gaucher, S. De, R.J. Smith, I.V. Shvets, S.K. Arora, G. Stanton, H.Y. Kim, K. Lee, G.T. Kim, G.S Duesberg, T. Hallam, J.J. Boland, J.J. Wang, J.F. Donegan, J.C. Grunlan, G. Moriarty, A. Shmeliov, R.J. Nicholls, J.M. Perkins, E.M. Grieveson, K. Theuwissen, D.W. McComb, P.D. Nellist and V. Nicolosi, *Science* ***331***, pp.568-571(2011).
8. M. Bera, Chandravati, P. Gupta and P.K. Maji, J. Nanosci. *Nanotechnol* ***18(2)***, pp. 902-912(2018).
9. A.A. Fikri, A.N. Aisyah, S. Alfarisa and W.S.B. Dwandaru, *AJAS* ***13(11)***, pp. 1129-1135(2016).
10. E. Varrla, K.R. Paton, C. Backes, A. Harvey, R.J. Smith, J. McCauley and J.N. Coleman, *Nanoscale* ***6***, pp. 11810-11819(2014).
11. M. Yi and Z. Shen, *Carbon* ***78***, pp. 622-626(2014).
12. M. Yi and Z. Shen, *J. Mater. Chem. A* ***3***, pp. 11700-11715(2015).
13. F.A. Mettler, W. Huda, T.T. Yoshizumi and M. Mahesh, *Radiology* ***248(1)***, (2008).
14. Y. Zheng, Y. Tang, Z. Bao, H. Wang, F. Ren, M. Guo, H. Quan and C. Jiang, *Int. J. Nanomedicine* ***10***, pp. 6435-6444(2015).
15. B. Gould, A. Greco, K. Stadler and X. Xiao, *Materials & Design* **117**, pp. 417-429(2017).
16. A. Ansón-Casaos, J. A. Puértolas, F. J. Pascual, J. Hernández-Ferrer, P. Castell, A. M. Benito, W. K. Maser, M.T. Martínez, Appl. Surf. Sci **301**, 264-272(2014).
17. L.F. Dumee, C. Feng, L. He, Z. Yi, F. She, Z. Peng, W. Gao, C. Banos, J.B. Davies, C. Huynh, S. Hawkins, M.C. Duke, S. Gray, P.D. Hodgson, L. Kong, *Carbon* ***70***, pp. 313-318(2014).
18. Y. Wang, Y. Feng, F. Mo, G. Qian, Y. Chen, D. Yu, Y. Wang and X. Zhang, *Appl. Phys. Lett* ***105***, 023102(2014).
19. L. Shahriary, A.A. Athawale, Bull. Mater. Sci **38(3)**, pp. 739-745(2015).
20. B. Zhang, L.Li, Z. Wang, S. Xie, Y. Zhang, Y. Shen, M. Yu, B. Deng, Q. Huang, C. Fan and J. Li, *J. Mater. Chem* ***22***, 7775(2012).
21. C. Suryanarayana and M.G. Norton, "X-Ray Diffraction", Plenum Press, New York, (1998).
22. D. Linden and T. B. Reddy, "Handbook of Batteries 3rd Ed", The McGraw Hill Companies Inc., (2002).
23. M.H. Khan, F. Gulshan and A.S.W. Kurny, *J. Inst. Eng. India Ser. D* ***94(1)***, pp. 51-56(2013).
24. S.V. Otari, M. Kumar, M.Z. Anwar, N.D. Thorat, S.K.S. Patel, D Lee, J.H. Lee, J.K. Lee, Y.C. Kang and L. Zhang, Scientific Reports. 7(1), 10980(2017).
25. I. Derkaoui, M. Khenfouch, I. Elmokri, S.J. Moloi, B.M. Mothudi, M.S. Dhlamini, M. Maaza, I. Zorkani and A. Jorio, Scientific Research. 5(1), pp. 14-24 (2016).
26. B. Rajagopalan and J.S. Chung, *Nanoscale Research Letters* ***9(5)***, pp. 35(2014).